PHYSICSAccess Research Paper
ISSN Online: 2756-3898, ISSN Print: 2714-500X https://doi.org/10.47514/phyaccess.sp.iss.2022.1.005

Optical Behaviour of Caffeine Mixed Perovskite Photoanode for Photovoltaic Application

Nicodemus Kure[1, 2], Muhammad Y Onimisi[2], Haruna Ali[2], Olumide O Ige[2] and Eli Danladi[3]

[1] Department of Physics, Kaduna State University, Kaduna, Kaduna State, Nigeria.
[2] Department of Physics, Nigerian Defence Academy, Kaduna, Kaduna State, Nigeria.
[3] Department of Physics, Federal University of Health Sciences, Otukpo, Benue State, Nigeria.

Corresponding E-mail: nicodemus.kure@kasu.edu.ng

Received 18-10-2022
Accepted for publication 22-11-2022
Published 28-11-2022

Abstract

Halide perovskites such as methylammonium lead triiodide ($CH_3NH_3PbI_3$) are attracting attention as energy-efficient light absorber materials for photovoltaic applications owing to their solution processing-power, tunable bandgap, strong absorption coefficients and cost-effectiveness. Scanning Electron Microscope (SEM) and Ultra-Violet Visible Spectroscopy (UV-vis) were used to characterize the prepared samples. The substrates were rinsed with propanol to remove impurities and later sintered before precursor deposition with different caffeine ratios via spray pyrolysis. The deposition method was used due to its homogenous ability. The SEM results indicate that the introduction of caffeine enhances nucleation, leading to an increase in the growth rate compared to the control. The UV-vis result shows a redshift to a higher wavelength, indicating an increase in visible light absorption which is attributed to the spectral overlap between the $CH_3NH_3PbI_3$ absorber and caffeine. The bandgap (Eg) energy analysis further confirmed that the caffeine-modified photoanode is a potential light absorber in perovskite solar cells application. This study provides a good understanding of the optical behaviour of caffeine-mixed perovskite photoanode nanostructures and a promising approach for photon energy management.

Keywords: Caffeine; Perovskite Solar Cells; Light Absorber; Scanning Electron Microscope; Wavelength

I. INTRODUCTION

Due to the global energy crisis, researches which are focused on renewable energy that are devoid of environmental pollution have received great attention within the scientific community for rapid economic development in the twenty-first century [1, 2]. Energy is one of the basic necessities of the present society. The abundance of solar energy cannot be overemphasized, which makes it one of the reliable and efficient energy sources that can meet global future energy demand [3, 4]. Thus, the photovoltaic (PV) industries are expected to provide a long-term solution to solve the energy and environmental problems by converting the solar energy into useable energy [3, 5, 6].

The PV solar cell is a device that converts sunlight energy into electricity via semiconductor materials. Semiconductor materials are responsible for the flow of electrons due to photoelectric effect leaving a hole that is filled by surrounding electrons [2]. The PV solar cells align the electrons in one direction, which forms a current [7] which is proportional to the number of absorbed photons, thereby making the PV solar cells to be a variable current source. However, the challenges that PV devices faced are cost; conversion power efficiency (PCE) and operating lifetime [8]. Researchers are now

focusing on finding materials that can overcome these challenges.

The technological evolution of PV solar cells started with the silicon (Si)-based solar cells which exhibited good PCE, high reliability and operating lifetime [9]. However, due to the high cost of Si and high material consumption, these have limited its development. Hence, the need to design new materials and processes that can give an equivalent PCE while at the same time reducing cost [2, 9]. Secondly, the emergence of thin films has reduced the cost of semiconductor material used to manufacture solar cells by half [10]. These solar cells were basically group III – IV elements; Cadmium Telluride (CdTe), Copper Indium Gallium Selenide (CIGS) and Gallium Arsenide (GaAs) solar cells [11, 12, 13, 14].

The third generation PV solar cells, were concentrators and organic-inorganic solar cells such as Dye-Sensitized Solar Cells (DSSCs), Organic Photovoltaic (OP), Quantum Dot Solar Cells (QDSCs) and Perovskite Solar Cells (PSCs) are cost effective compared to other older generations [4, 15]. Organic-inorganic hybrids PSCs have attracted much attention due to their PCE in comparative with that of the commercial Si-based solar cells. The first report of solar cell with perovskite absorber employing a liquid electrolyte showed a 3.8% of total PCE of perovskite sensitized solar cell [1]. The PCE was further enhanced to 9.7% [16]. However, PSCs that possess high PCE contain organic cation amongst such are Methyl-ammonium (MA^+) and Formamidinium (FA^+), which reduces the device long-term stability [15]. Nevertheless, the corrosive nature of liquid electrolyte enables the perovskite material to dissolve within few minutes of device operation. Hence, a shift to solid-state type has enhanced the PCE of such PCSs to exceed 25%, approaching 26.7% of crystalline silicon-based solar cells [8, 15, 17].

PSCs has exceptional properties which significantly attract scientific community attention among such are; adjustable direct band gap, long charge carrier diffusion length, highly efficient ambipolar charge transport, low-cost of production, defect tolerance, wide optical absorption and large absorption coefficients [3, 15, 18]. Thus, potentially, thin-film PSCs technology could be highly competitive to Si-based materials which attract most consumers in the market [17]. Among the application PSCs are in field-effect transistors [19], nonlinear optical materials [20], lasing [21] and light-emitting diodes [22]. Additionally, PSCs can be prepared in the common laboratories via relative temperature solution process methods such as spraying, ultrasonic spraying, chemical vapor deposition, blade coating, spin coating and screen printing [3, 17]. Lastly, the PSCs device structure can be categorized such as planar PSCs, mesoporous PSCs and inverted PSCs [23].

This research intends to look into the optical behavior of Caffeine Mixed Perovskite Photoanode by modifying the absorber with an organic substance (Caffeine), which invariably would replace the conventional organic Hole Transport Layer (HTL) Spiro-OMeTAD with HTL free architecture due to its hygroscopic nature. Caffeine is an organic substance belonging to alkaloid class with exceptional properties, among such are: non-volatile molecular formula $C_8H_{10}N_4O_2$, melting point of $237\ °C$ and density of $1.05\ g/cm^3$. The caffeine will molecularly lock the precipitation of trigonal PbI at elevated temperatures, by strongly interacting with Pb^{2+} in reducing the PSCs crystals growth, which reduces the defect density. Thus, the caffeine serves as thermal enhanced material, which also reduce the rate of moisture content attack on the perovskite absorber.

II. Materials and Numerical Method

A. Materials

All chemicals are industrial grade and were used without further purification. The chemicals include: Dense Titanium (IV) Isopropoxide by Sigma-Aldrich Chemical Company Ltd.; Methylammonium Iodide by Solaronix; Amosil 4R by Solaronix; Titanium nanoxide D/sp by Solaronix; Zirconium nanoxide Z/sp by Solaronix; Acetyl-acetone by Guangdong Guanhua Sci-Tech Company Ltd; Caffeine by Sigma-Aldrich Chemical Company Ltd.; Lead (II) Iodine by Sigma-Aldrich Chemical Company Ltd.; Elcocarb by Solaronix; Glass slides and TiO_2 paste (Dyesol 18NR-T).

B. Methods

1) Preparation Methods

The glass slides were cut gently into a fine square shape using an electric hand engraver with area dimensions of $2.5\ cm \times 2.5\ cm$. Afterward, the glass slides were sonicated for about 1 minute to remove impurities, then rinsed with distilled water to remove excess fumes. Lastly, the glass slides were heated via magnetic stirrer plate at 76 ºC. The temperature was monitored using an infrared thermometer for 5 minutes.

2) Deposition Methods

The TiO_2 paste was dispersed in ethanol (TiO_2 paste to ethanol volume ratio of 1:3). The TiO_2 films was prepared using a modified sol–gel method, in which $2\ g$ of P25 (Dagusta) TiO_2 powder was dissolved in 10 ml of deionized water mixed with $0.2\ mole$ of Triton-X 100 and $0.4\ g$ of acetaldehyde, then vibrated ultrasonically for 24 hours. The deposition of compact titanium oxide c-TiO_2 layer which is sometimes referred to as blocking or dense layer is crucial in achieving high PCEs by preventing recombination processes [15, 24]. The technique used in the deposition process is Spray pyrolysis, where the c-TiO_2 colloid precursor was deposited homogenously at 480 °C for about 3.04 seconds, which form an important part of Electron Transport Layer (ETL) [25]. The TiO_2 liquid paste was spin-coated on the glass slide substrate via modified centrifuge machine at 3000 rpm for 15 seconds. The samples were annealed at 500 °C for 30 minutes after deposition. Samples colour changes from white to brownish colours, then translucent as the temperature increases. After cooling at room temperature, the samples were collected as m-TiO_2. The annealing process allows the titanium dioxide

nanocrystals to partially dissolve together, which basically ensures good electrical contact as well as mechanical adhesion to the glass substrate. The deposited c-TiO_2 and m-TiO_2 were dried at 150 °C for 5 minutes. This one-step annealing process, both blocking and mesoporous were annealed together at 500 °C for 30 minutes, which was beneficial to the improvement of the interfacial contact. Screen printing was used in the deposition process with a mesh count of 70 ($\times$ 1 m per square feet). The Zirconium nanoxide (ZrO_2) paste was meshed about $\times$ 1 m per square feet on the substrate glass and annealed at 500 °C for 5 minutes to avoid peeling and agglomeration. The sample changes its colour during the annealing process, from white to brown then back to white as the temperature increases.

3) Characterization Methods

The surface morphologies were observed by Scanning Electron Microscopy (Phenom Pro X model, Eindhoven de Netherlands) operated at an acceleration voltage of 10 KV. Optical spectra were examined and characterized by means of ultraviolet–visible light (UV–vis) spectrometer (Axiom Medicals UV752 UV-vis-NIR). Thickness measurement of the functionalized materials was obtained with a Dektac 150 surface profiler.

III. Results and Discussion

The image of the control sample film in Fig. 1 (a) shows a denser surface with shinning particles observed due to electron backscattering [26]. Fig. 1 (b) shows the SEM image of sample with 0.3 ml caffeine. From the image, the shiny surface contains granular shiny structure of introduced caffeine, thereby improving the charge extraction efficiency in the films [27]. The shiny particles show that caffeine can scattered incident light to increase light absorption surface area. Putting, 0.3 ml of caffeine results to decrease in recombination rate which is related to the grain boundaries. The Image J computing software shows that the grain sizes are bigger in sizes compare to the Fig. 1 (a) which further entails the possibility of having a decrease in the charge recombination [28, 29]. Fig. 1 (c) show typical SEM images of the top surface morphology of the perovskite absorber formed with 0.6 ml of caffeine. Lastly, Fig. 1 (d) show SEM image of the top surface morphology of the perovskite absorber with 0.9 ml of caffeine, a smaller grain size indicating a lesser grain boundary which could lead to low charge extraction efficiency of the films. The result is similar to that in other literatures [15]. The presence of agglomerated shinny surfaces was observed which may have come up during the sintered process.

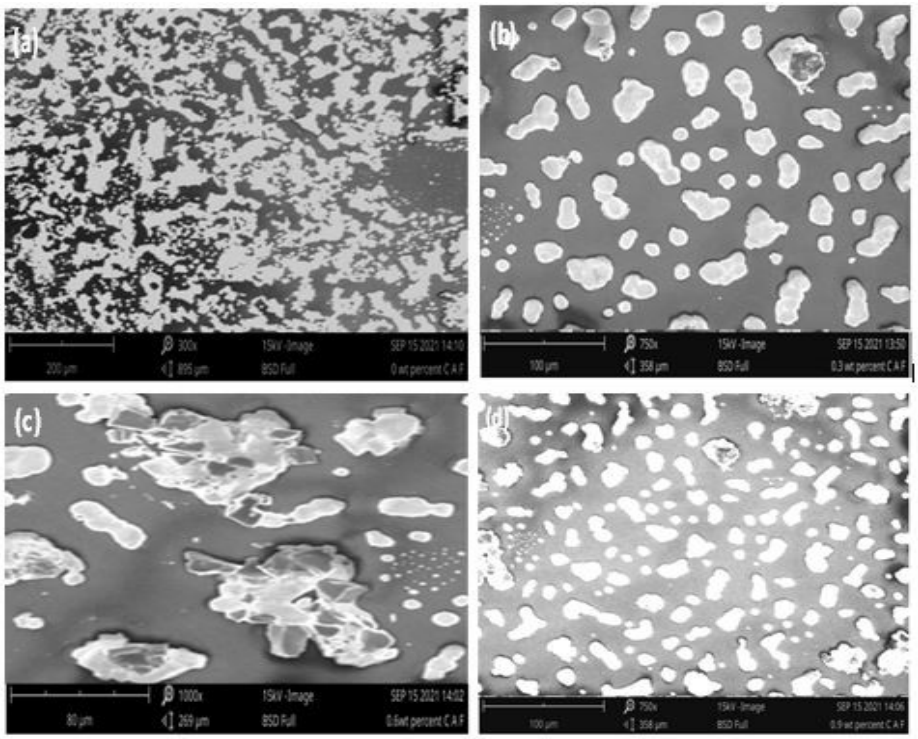

Fig. 1 Showing SEM image of (a) control sample, (b) sample with 0.3 ml caffeine, (c) sample with 0.6 ml caffeine, (d) sample with 0.9 ml caffeine.

Fig. 2 show the absorbance-wavelength plot of samples with and without caffeine at different amounts. The sample without caffeine is in Fig. 2(a), while caffeine-containing samples are in Fig. 2(b) - (d). A redshift was observed, indicating an increase in visible light absorption which is attributed to the spectral overlap between the $CH_3NH_3PbI_3$ absorber and caffeine was monitored using UV-extinction spectra [25, 30, 31]. Absorption peaks were observed at 346, 384, 418, 663 and 959 nm with absorbance heights at ~1.19, ~1.47, ~1.38, ~ 0.67 and ~ 0.45 respectively in Fig. 2(b). Absorption was exhibited at 386, 421, 660 and 961 nm with absorbance height of ~1.42, ~1.35, ~0.73 and ~0.48 respectively in Fig. 2(c), which shows a slight blue shift at the absorbance. Also, absorbance was exhibited at 252, 386 and 663 nm with absorbance height of ~1.42, ~1.35 and ~0.73 respectively but a broad peak was observed around (907 - 961) nm with absorbance height of ~ (0.35 - 0.35) respectively in Fig. 2(d) which shows a slight blue shift at the resonance. This shift was attributed to the increase of the effective dielectric function of the medium surrounding the caffeine thereby achieving higher surface adsorption. The relatively broad and strong enhancement is observed in the range of 350 - 700 nm with a maximum enhancement around 400 nm. This enhanced absorption and broadened spectra absorption range of the photoanodes were mainly attributed to the caffeine. This enhanced electromagnetic field contributes to enhancing the light harvesting capacity of the perovskite films.

As observed, a significant shift of the absorption peak toward the visible and the near infrared regions of the solar spectrum for caffeine modified composite, exhibiting a maximum at around 400 - 500 nm wavelength and an enlargement of the absorption band (the so-called “tail” of the band) was observed, suggesting an increase of the photo catalytic activity within the visible range. Thus, more content of light will be scattered as caffeine are used for light scattering in PSC devices.

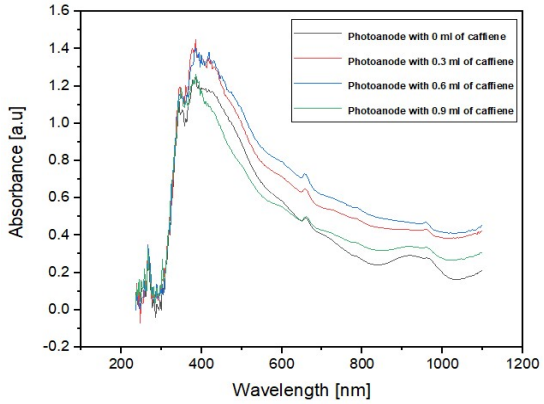

Fig. 2 Shows the UV-vis spectroscopy of the combined plots for the modified and unmodified samples.

Fig. 3 compares the optical transmission of the different prepared caffeine modified samples. The spectrum without nanoparticles as a reference is also included. It was observed that at wavelengths between 544 nm and 1000 nm, sample with 0.9 ml of caffeine transmitted slightly higher than the reference sample while samples with 0.3 ml and 0.6 ml transmitted slightly below the reference sample. This result shows that, the TiO_2 index of refraction is more dispersive than that of caffeine nanoparticles modified samples in the wavelength region [32]. The reference photoanode experiences a relatively short fall around 800 nm and 1000 nm but maintains a constant transmission above 566 nm. At longer wavelength, for all the photoanodes with caffeine NPs, a rise in transmittance within 600 to 1100 nm was observed and it remains constant within the region. Below 600 nm, a sharp fall in transmittance was noticed. The difference in observed transmittance of films may be ascribed to disparity in surface morphologies, crystallite size and existence of surface defects causing a decrease in transmittance to scattering of light. These combinations of the physical mechanisms caused the peaks in some of the results shown in Fig. 3. From the analysis of the transmission values in the nanoparticle structures, several effects give the enhancements of optical transmissions in mixing caffeine nanoparticle structures.

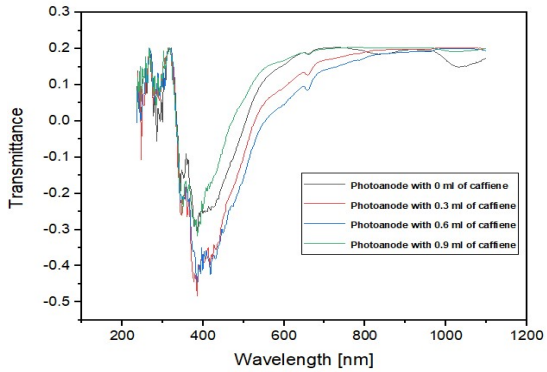

Fig. 3 showing the combined optical transmission of the prepared samples.

A strong scattering contribution (reflectance) from caffeine clusters within the range of 400 - 1100 nm was observed (see Fig. 4) as reported in [33]. The redshift and broadening of the main scattering band is ascribed to the caffeine nanoparticles forming the clusters and to inter-cluster coupling influence [34, 35]. However, the reflectance spectra when light is incident differ substantially, as shown in the structures with caffeine nanoparticles at different locations.

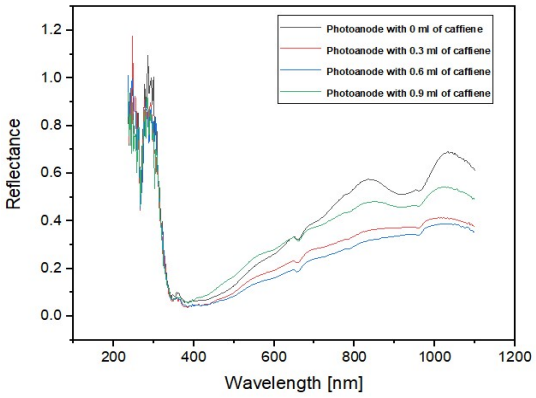

Fig. 4 The combined optical reflectance of the prepared samples.

The optical energy band gap of the as prepared TiO_2 films were estimated at the intercept of zero y-axis of linear extrapolation of the plot to enable us know whether the most favourable transition for the functionalized nanoparticle is direct or indirect energy band gap. The $CH_3NH_3PbI_3$ has a band gap energy of 1.66 eV which agrees with similar experimental results of 1.50 eV obtained in [1, 36, 37, 38, 39, 40] and theoretical result of 1.64 eV obtained in [41]. A reduction in E_g from 2.03 eV to 1.95, 1.99 and 1.93 eV respectively for samples with 0.3, 0.6 and 0.9 ml of caffeine were observed (see Fig. 5). This reduction in energy band gaps is mainly attributed to the increased in grain size which resulted from the increased of thickness. This inherently has established the phenomenon of quantum size effect whereby the smaller the grain sizes the higher the energy band gap [42].

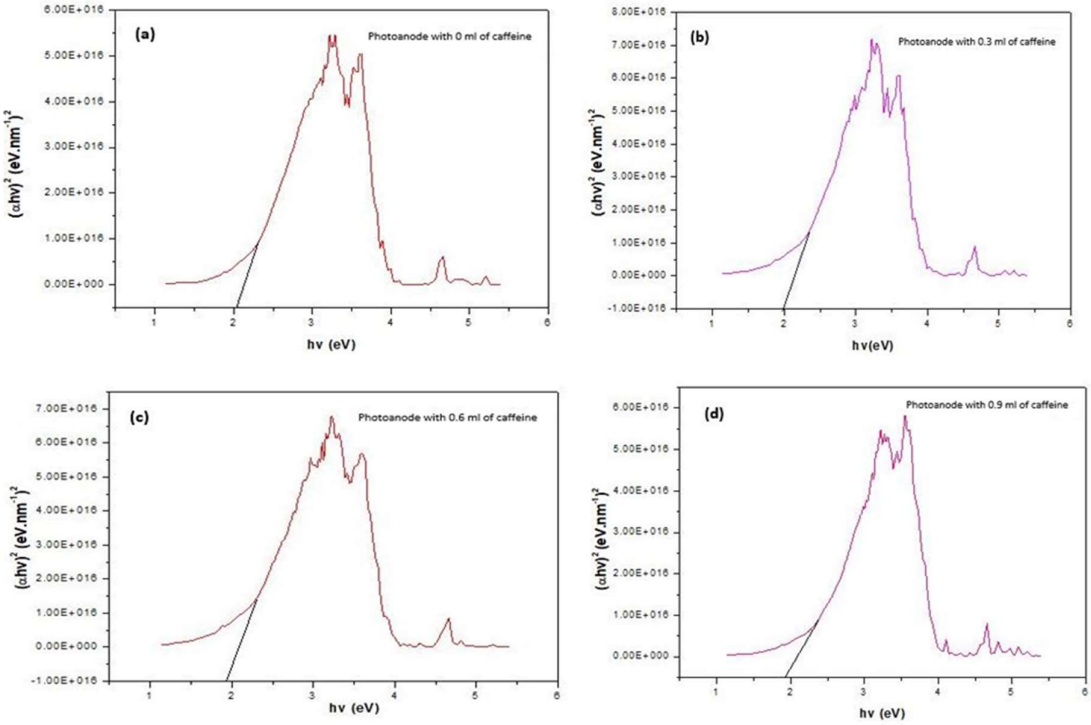

Fig. 5 The optical energy band gap of the prepared samples.

IV. CONCLUSION

Optical behaviour of the as prepared samples were investigated via SEM and UV-vis, and the modification of caffeine nanoparticles (NPs) were systematically examined. Results obtained, indicate the positive effects of caffeine were maximized by controlling the mole of caffeine deposited on photoanode layer. These results offer a possible method that could be used to enhance the optical absorption of solar cells materials by employing organic nanostructures.

References

[1] A. Kojima., K. Teshima, Y. Shirai, and T. Miyasaka, "Organometal Halide Perovskites as Visible-Light Sensitizers for Photovoltaic," J. of the American Chem. Society, vol. 131, pp. 6050–6051, 2009.

[2] T. Ma, S. Wang, Y. Zhang, K. Zhang, and L. Yi, "The development of all-inorganic $CsPbX_3$ perovskite

solar cells," J. of Materials Sci., vol. 5, no. 2, pp. 464–479, 2019.
[3] M. J. You et al., "A review of aspects of additive engineering in perovskite solar cells," Adv. Energy Materials, vol. 4, no. 1, pp. 1–16, 2020.
[4] M. Shahiduzzaman, S. Fukaya, E. Y. Muslih, L. Wang, M. Nakano, M Akhtaruzzaman, M. Karakawa, K Takahashi, et al., "Metal oxide compact electron transport layer modification for efficient and stable perovskite solar cells," Materials, vol. 13, no. 9, pp. 1-19, 2020.
[5] S. Nair, S. B. Patel, and J. V. Gohel, "Recent trends in efficiency-stability improvement in perovskite solar cells," Materials Today Energy, vol. 17, pp. 100-449, 2020.
[6] Z. Yang, B. H. Babu, S. Wu, T. Liu, S. Fang, Z. Xiong, L. Han, and W. Chen, "Review on Practical Interface Engineering of Perovskite Solar Cells: From Efficiency to Stability," Solar RRL, vol. 4, no. 2, pp. 1–16, 2020.
[7] M. H. Li, P. S., Shen, K. C., Wang, T. F., Guo, and P. Chen, "Erratum: Inorganic p-type contact materials for perovskite-based solar cells," J. of Materials Chemistry A, vol. 3, no. 17, pp. 9318–9319, 2015.
[8] S. F. Hoefler, G. Trimmel, and T. Rath, "Progress on lead-free metal halide perovskites for photovoltaic applications: a review," Monatshefte Fur Chemie, vol. 148, no. 5, pp. 795–826, 2017
[9] NREL, "Best Research-Cell Efficiency Chart" https://www.nrel.gov/pv/assets/pdfs/best-research-cell-efficiencies.20190802.pdf, 2019.
[10] N. Kumar, J. Rani, and R. Kurchania, "A review on power conversion efficiency of lead iodide perovskite-based solar cells," Materials Today: Proceedings, xxxx., 2020.
[11] M. A. Green, A. Ho-Baillie, and H. J. Snaith, "The emergence of perovskite solar cells," Nature Photonics, vol. 8, no. 7, pp. 506–514, 2014.
[12] C. Liu, M. Wu, Y. Wu, D Wang, and T. Zhang, "Efficient All-Inorganic $CsPbI_2Br$ perovskite solar cell with carbon electrode by revealing crystallization kinetics and improving crystal quality," Journal of Power Sources, vol. 447, pp. 227-389, 2020.
[13] P. Roy, K. S. Numeshwar, T. Sanjay, and K. Ayush, "A review of aspects of additive engineering in perovskite solar cells," Solar Energy, vol. 198, pp. 665–688, 2020.
[14] S. Yang, L. Wang, L. Gao, J. Cao, Q. Han, F. Yu, Y. Kamata, et al., "Excellent Moisture Stability and Efficiency of Inverted All-Inorganic $CsPbIBr_2$ Perovskite Solar Cells through Molecule Interface Engineering," ACS Applied Materials and Interfaces, vol. 12, no. 12, pp. 13931–13940, 2020.
[15] R. Wang, M. Mujahid, Y. Duan, Z. K. Wang, J. Xue, and Y. Yang, "A Review of Perovskites Solar Cell Stability," Advanced Functional Materials, vol. 2019, pp. 1808843, 2019.
[16] J-H. Im, H-S. Kim, C-R. Lee, K-B. Lee, T. Moehl, A. Marchioro, S-J. Moon, and R. Humphry-Baker, "Lead Iodide Perovskite Sensitized All-Solid-State Submicron Thin Film Mesoscopic Solar Cell with Efficiency Exceeding 9%," Scientific Reports, vol. 591, no. 2, pp. 1–10, 2012.
[17] M. Wu, N. Haji Ladi, Z. Yi, H. Li, Y. Shen, and M. Wang, "Stability Issue of Perovskite Solar Cells under Real-World Operating Conditions," Energy Technology, vol. 8, no.4, pp. 1–12, 2020.
[18] H. D. Pham, T. C. J. Yang, S. M. Jain, G. J. Wilson, and P. Sonar, "Development of Dopant-Free Organic Hole Transporting Materials for Perovskite Solar Cells," Advanced Energy Materials, vol. 10, no. 13, pp. 1903326, 2020.
[19] E. Shi, Y. Gao, B. P. Finkenauer, A. Akriti, A. H. Coffey, and L. Dou, "Two-dimensional halide perovskite nanomaterials and heterostructures," Chemical Society Reviews, vol. 47, no. 16, pp. 6046–6072, 2018.
[20] J. Yi, L. Miao, J. Li, W. Hu, C. Zhao, and S. Wen, "Third-order nonlinear optical response of $CH_3NH_3PbI_3$ perovskite in the mid-infrared regime," Optical Materials Express, vol. 7, no. 11, pp. 38-94, 2017.
[21] R. Dhanker, A. N. Brigeman, A. V. Larsen, R. J. Stewart, J. B. Asbury, and N. C. Giebink, "Random lasing in organo-lead halide perovskite microcrystal networks," Applied Physics Letters, vol. 105, no. 15, pp. 151-112, 2014.
[22] K. Lin, J. Xing, L. N. Quan, F. P. G. de Arquer, X. Gong, J. Lu, L. Xie, W. Zhao, et al., "Perovskite light-emitting diodes with external quantum efficiency exceeding 20 per cent," Nature, vol. 562, no. 7726, pp. 245–248, 2018.
[23] X. Qin, Z. Zhao, Y. Wang, J. Wu, Q. Jiang, and j. You, "Recent progress in stability of perovskite solar cells," J. of Semiconductors, vol. 38, no. 1, pp.011-002, 2017.
[24] P. J. Cameron, and L. M. Peter, "Characterization of Titanium Dioxide Blocking Layers in Dye-Sensitized Nanocrystalline Solar Cells," Journal of Physical Chemistry B, vol. 107, no. 51, pp. 14394–14400, 2003.
[25] M. Y. Onimisi, D. Eli, S. G. Abdu, H. O. Aboh and J. Ezeoke, "Size effects of silver nanoparticles on the photovoltaic performance of dye sensitized solar cells," American Chemical Science Journal, vol. 13, no.3, pp. 1-8, 2016.
[26] B. Yu, K. M. Leung, Q. Guo, W. M. Lau, and J. Yang, "Synthesis of Ag-TiO2 composite nano thin film for antimicrobial application," Nanotechnology, vol. 22, pp. 1-9, 2011.
[27] D. H. Wang, D. Y. Kim, K. W. Choi, J. H. Seo, S. H. Im, J. H. Park, O. O. Park, and A. J. Heeger, "Enhancement of Donor-Acceptor Polymer Bulk

Heterojunction Solar Cell Power Conversion Efficiencies by Addition of Au Nanoparticles," Angewandte Chemie, vol. 50, no. 24, pp. 5519-5523, 2011.

[28] J. Alonso, R. Diamant, P. Castillo, M. C. AcostaeGarcı´a, N. Batina, and E. Haro-Poniatowski, "Thin films of silver nanoparticles deposited in vacuum by pulsed laser ablation using a YAG: Nd laser," Applied Surface Science, vol. 255, pp. 4933-4937, 2009.

[29] Y. Shao, Z. Xiao, C. Bi, Y. Yuan, and J. Huang, "Origin and Elimination of Photocurrent Hysteresis by Fullerene Passivation in $CH_3NH_3PbI_3$ Planar Heterojunction Solar Cells," Nature Communications, vol. 5, pp. 57-84, 2014.

[30] D. Eli, P. M. Gyuk, A. A. Kassimu, M. S. Ahmad, A. Francis, and N. Kure, "Photoelectrochemical Cell Based on Betalain Pigment and TiO_2 Nanoparticles for Exploring Solar Energy Concept," Journal of the Nigerian Association of Mathematical Physics, vol. 37, pp. 307-312, 2017.

[31] D. Eli, G. J. Ibeh, O. O. Ige, J. A. Owolabi, R. U. Ugbe, B. O. Sherifdeen, M. Y. Onimisi, and H. Ali, "Silver Nanoparticles as Nano Antenna for TiO_2 Activation and its Application in DSSC for Enhanced Performance," J. of Theoretical and Applied Physics, vol. 1, no. 3, pp. 88–98, 2019.

[32] Y-M. Yeh, Y-S. Wang, and J-H. Li, "Enhancement of the optical transmission by mixing the metallic and dielectric nanoparticles atop the silicon substrate," Optics Express, vol. 19, no.2, pp. 80-94, 2011.

[33] T. J. Antosiewicz, and T Tarkowski, "Localized surface plasmon decay pathways in disordered two-dimensional nanoparticle arrays," ACS Photonics, vol. 2, no. 12, pp. 1732-1738, 2015.

[34] N. Pazos-Perez, C. S. Wagner, J. M. Romo-Herrera, L. M. Liz-Marzan, F. J. Garcia deAbajo, A. Wittemann, A. Fery, A. Alvarez-Puebla, "Organized plasmonic clusters with high coordination number and extraordinary enhancement in surface-enhanced raman scattering (SERS)," Angew Chemie (International Ed. In English), vol. 51, no. 51, pp. 12688–12693, 2012.

[35] F. L. Yap, P. Thoniyot, S. Krishnan, and S. Krishnamoorthy "Nanoparticle cluster arrays for high-performance sers through directed self-assembly on flat substrates and on optical fibers," ACS Nano, vol. 6, no. 3, pp. 2056-2070, 2012.

[36] J. Burschka, N. Pellet, S-J. Moon, R. Humphry-Baker, P. Gao, M. K. Nazeeruddin, and M. Gratzel, "Sequential Deposition as a Route to High-Performance Perovskite-Sensitized Solar Cells," Nature, vol. 499, pp. 316−319, 2013.

[37] M. Liu, M. B. Johnston, and H. J. Snaith, "Efficient Planar Heterojunction Perovskite Solar Cells by Vapour Deposition," Nature, vol. 501, pp. 395−398, 2013.

[38] L. Etgar, P. Gao, Z. Xue, Q Peng, A. K. Chandiran, B. Liu, Md. K. Nazeeruddin, and M. Gratzel, "Mesoscopic $CH_3NH_3PbI_3/TiO_2$ Heterojunction Solar Cells" J. of the American Chem. Society, vol. 134, pp. 17396−17399, 2012.

[39] H-S. Kim, C-R. Lee, J-H. Im, K-B. Lee, T. Moehl, A. Marchioro, S-J. Moon, R. Humphry-Baker, et al., "Lead iodide perovskite sensitized all-solid-state submicron thin film mesoscopic solar cell with efficiency exceeding 9%," Scientific Reports, vol. 2: 591, 2012.

[40] M. M. Lee, J. Teuscher, T. Miyasaka, T. N. Murakami, and H. J. Snaith, "Efficient Hybrid Solar Cells Based on Meso-Superstructured Organometal Halide Perovskites," Science, vol. 338, pp. 643−647, 2012.

[41] G. Giorgi, J-I. Fujisawa, H. Segawa, and K. Yamashita, "Small Photocarrier Effective Masses Featuring Ambipolar Transport in Methylammonium Lead Iodide Perovskite: A Density Functional Analysis," J. of Physical Chemistry Letters, vol. 4, pp. 4213−4216, 3013.

[42] M. Oztas, "Influence of Grain Size on Electrical and Optical Properties of InP Films," Chinese Physics Letters, vol. 25, no. 11, pp. 4090-4092, 2008.